JOURNAL OF CATALYSIS 133, 124–135 (1992)

The Effect of Modifying Alumina with Sulfate and Phosphate on the Catalytic Properties of Mo/Al_2O_3 in HDS Reaction

SEO IL KIM AND SEONG IHL WOO[1]

Department of Chemical Engineering, Korea Advanced Institute of Science and Technology, P.O. Box 150, Cheong-Ryang, Seoul, Korea

Received January 17, 1991; revised August 19, 1991

The properties of alumina modified with sulfate (Al–S) and phosphate (Al–P) and Mo catalysts supported on modified alumina (Mo/Al–P and Mo/Al–S) were characterized by IR, XRD, DRS, ESR, temperature-programmed sulfidation (TPS), and the oxygen chemisorption. Catalytic activities of Mo/Al–P and Mo/Al–S were evaluated in the thiophene HDS reaction. The point of zero charge (PZC) of the modified alumina and the amount of Mo adsorbed on modified alumina decreased with increasing modifier content. The bonding mode of sulfate on alumina changed with increasing sulfate content. The decrease in the PZC of Al–P and in the number of the adsorption sites for Mo anions on Al–P facilitated the formation of polymolybdate on Mo/Al–P. The sulfidation of Mo catalyst was also promoted in Mo/Al–P. The catalytic activity in the thiophene HDS reaction of phosphate-modified catalysts was higher than that of Mo/Al_2O_3 when the phosphate content was less than 5 wt%. Bulk MoO_3 was formed more easily in Mo/Al–S than in Mo/Al–P. The suppression of the sulfidation of Mo/Al–S may be explained by the formation of bulk MoO_3 and the presence of the S=O group. The HDS activity of sulfate-modified catalysts was lower than that of Mo/Al_2O_3, regardless of the sulfate content.

INTRODUCTION

Alumina has been used as a support for hydrodesulfurization (HDS). The interaction between Mo and alumina is known to influence the structure and activity of HDS catalyst based on Mo (*1–3*). The strong interaction between Mo and alumina facilitates the formation of a monolayered rather than a multilayered Mo structure, resulting in higher dispersion of Mo on the support (*1*). The interaction between Mo and alumina may decrease the HDS activity because of the potential suppression of the molybdate sulfidation (*2*). On the other hand, Mo sulfide that interacts strongly with alumina has a lower intrinsic activity as compared with weakly interacting Mo sulfide (*3*).

The interaction between Mo and alumina is the result of a reaction between Mo anion and the basic (protonated) hydroxyl groups on the alumina surface during the catalyst preparation (*4–6*). The molybdate adsorption on the alumina surface might occur by the decomposition of the adsorbing molecules/ion and physisorption on coordinatively unsaturated (cus) Al^{+3} sites (*4, 5*). It is therefore suggested that the interaction between Mo and alumina may be affected by the surface properties of alumina. Recently, a number of reports about the γ-alumina/electrolyte interface suggested that the electrical properties of the alumina surface may be regulated by changing parameters such as the solution pH and temperature and the kind of ionic dopants (*6–10*). More specifically the effect of ions such as F^-, Cl^-, Na^+, Li^+, and Mg^{2+} on the electrified interface of γ-alumina in aqueous electrolytes containing molybdate species has been thoroughly investigated (*10–13*). Despite the report that phosphate affects both the adsorption of anionic Mo species (*14, 15*)

[1] To whom correspondences should be addressed.

0021-9517/92 $3.00

TABLE 1

The Specific Surface Area of Modified Alumina

Support	Area (m^2/g)	Support	Area (m^2/g)
Al_2O_3	220	—	—
Al–P(1)	195	Al–S(1)	190
Al–P(3)	180	Al–S(3)	180
Al–P(5)	162	Al–S(5)	175
Al–P(10)	149	Al–S(10)	151

and the properties of calcined and sulfided Mo/Al_2O_3 catalyst (*16–19*), phosphate is known to have a beneficial effect on HDS (*20–22*). This beneficial effect of the phosphate is attributed to the increase of the Mo dispersion (*20*), less deactivation (*21*), or the increase in the amount of the octahedral Co or Ni (*20, 22*). For a better understanding concerning the role of phosphate, it is necessary to investigate the calcined and sulfided state of Mo catalyst supported on the alumina modified with the phosphate (Mo/Al–P).

In the present study, the surface properties of the alumina modified with phosphate and sulfate were investigated by IR and PZC measurements. The Mo/Al–P and Mo/Al–S catalysts were characterized by DRS, XRD, ESR, TPS (temperature-programmed sulfidation), and oxygen chemisorption and their catalytic activities were determined using the HDS of thiophene as a probe reaction.

EXPERIMENTAL

Preparation of Mo Catalysts

γ-Alumina (Strem Chem. Co.) was used for the preparation of modified alumina. The pore volume and surface area of the pure alumina were 0.25 cm^3/g and 220 m^2/g, respectively. The modified alumina was prepared by impregnating γ-alumina with aqueous solutions of phosphoric acid (Hayashi Co.) or ammonium sulfate (Tokyo Kasei Co.), drying it at 393 K for 6 h, and calcining at 773 K for 6 h. The surface areas of modified aluminas are listed in Table 1. The Mo catalyst was prepared by the incipient wetness method with ammonium heptamolybdate (Strem Chem. Co.). After impregnation, the Mo catalyst was dried at 373 K for 6 h and calcined at 773 K for 6 h. The Mo content in the catalysts was 10 wt%. Al–$M(x)$ denotes the modified alumina, with M representing the kind and x the content (wt%) of modifier, either PO_4 or SO_4.

Point of Zero Charge (PZC) and Mo Uptake Measurement

The PZC of modified alumina was determined by a drift method (*11*). The pH's of several samples of deionized water were adjusted to various pH values with HNO_3 or NH_4OH. Samples of modified alumina (0.2 g) were poured into these solutions (25 ml). The final pH's were measured after 24 h. The difference between initial pH and final pH, ΔpH, was obtained. Plots of ΔpH vs initial pH of modified alumina were made and the PZCs of modified alumina were determined as the point at which ΔpH was equal to zero.

Adsorption experiments were performed in aqueous Mo solution of which the Mo concentration and pH were 1 mg Mo/cm^3 and 6.0, respectively. Ammonium heptamolybdate was used for the preparation of Mo solution. A total of 0.2 g of modified alumina was poured into 25 ml of aqueous Mo solution and left for 24 h. The amounts of Mo anion adsorbed on the modified alumina were determined by measuring the difference between initial and final Mo concentration in Mo solution. Mo concentration in solution was measured by AA (atomic absorption: Varian Aerograph Co. Model 575).

IR

The IR spectra of the samples were recorded in transmittance mode with an IR spectrophotometer (Bomem Inc., Michelson-102). The resolution was 4 cm^{-1} and the scan number was 64. A self-supporting wafer was prepared by pressing 15 mg powdered sample at 15,000 psi and was loaded on a sample holder of the IR cell. After the

sample was evacuated at 10^{-4} Torr at 773 K for 2 h and then cooled to room temperature *in vacuo*, the IR spectra of the calcined state were recorded. Pyridine was adsorbed on the wafer at 423 K for 1 h and evacuated at 423 K and 10^{-4} Torr for 2 h. The IR spectra were recorded at room temperature.

DRS

The diffuse reflectance spectra of the calcined Mo catalysts were recorded using a diffuse reflectance spectrometer (Shimazu Co.) in the 200–400 nm range. MgO was used as a reflectance reference.

XRD

The XRD spectra of the calcined Mo catalysts were recorded using an X-ray diffractometer (Rigaku Co.) equipped with a Cu X-ray tube. The tube voltage and current were 35 kV and 15 mA, respectively.

ESR

The ESR spectra of the Mo catalysts sulfided at 673 K for 2 h were taken at room temperature using an ESR spectrometer (ER 200D-SRC, Bruker Co.), which has a single cavity and was operated in X-band microwave frequency (9.45 GHz). α,α-Diphenyl-β-picrylhydrazyl (DPPH) has been used to calibrate the g factor. An *in situ* ESR quartz reactor with a side-arm tube was designed to avoid air contact (*23*). To remove physisorbed species, sulfided catalysts were evacuated at 10^{-1} Torr for 10 min at room temperature.

Oxygen Chemisorption

An oxygen chemisorption experiment on sulfided Mo catalysts was performed by a dynamic adsorption method using a GC equipped with TCD. The catalyst sulfided at 673 K for 2 h was flushed for 0.5 h and cooled to 303 K in N_2. A pulse of a known volume of oxygen was introduced by a six-port valve until the peak area of the oxygen effluent had a constant value within 1%.

Temperature-Programmed Sulfidation

The samples were calcined at 773 K for 2 h and cooled to room temperature with He. Calcined samples were exposed to the sulfiding gas (20 cm^3) until the signal was stabilized. The sulfiding gas was composed of 4% H_2S, 16% H_2, and 80% He. After the stabilization was reached, the samples were heated to 1073 K with a rate of 10 K min^{-1}. The effluents were analyzed by mass spectrometer (VG Quadrupoles Co., SX-300). This experimental method was recently applied to study the sulfidation process of the HDS catalyst (*24, 25*).

Thiophene Hydrodesulfurization

The Mo catalysts were presulfided by heating 0.2 g of samples to 673 K in N_2 for 0.5 h. Subsequently they were sulfided with a mixed flow (40 cm^3/min) of 10% H_2S (Matheson CP grade) and 90% H_2 (Matheson UHP grade) for 2 h. The sulfided catalysts were flushed with N_2 for 0.5 h and cooled to the reaction temperature (573 K). The flow rate of thiophene (99%$^+$, Aldrich) was 6.55×10^{-5} mol/min and the mole ratio of H_2/thiophene was 18. Steady state was achieved after 2 h. Reaction products were analyzed by GC (Varian Aerograph Co. Model 920) equipped with OV-101 column.

RESULTS

PZC and Mo Uptake Measurement

The PZC of pure alumina was found to be at pH 8.3 as shown in Fig. 1. The PZC of alumina modified with sulfate rapidly decreased to 6.1 when 1 wt% of sulfate was added and then slowly decreased to 3.4 with increasing sulfate content to 10 wt%. The PZC of alumina modified with phosphate, on the other hand, decreased slowly to 6.5 with increasing phosphate content to 10 wt%. The amounts of Mo uptake on modified alumina were found from adsorption experiments. Typical results are shown in Fig. 2. The amount of Mo uptake on pure alumina was found to be equal to 4.02 Mo wt% and it decreased with increasing modifier content.

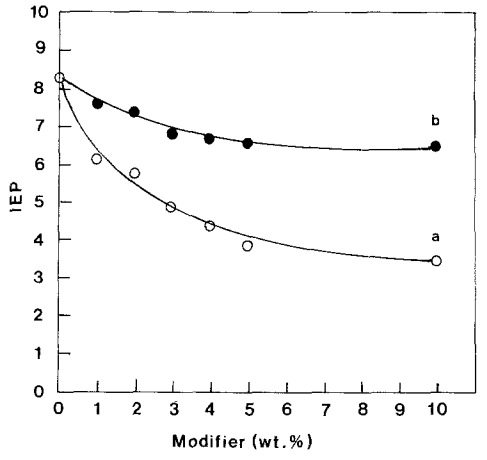

FIG. 1. The PZCs of alumina modified with various contents of modifier: (a) Al–S and (b) Al–P.

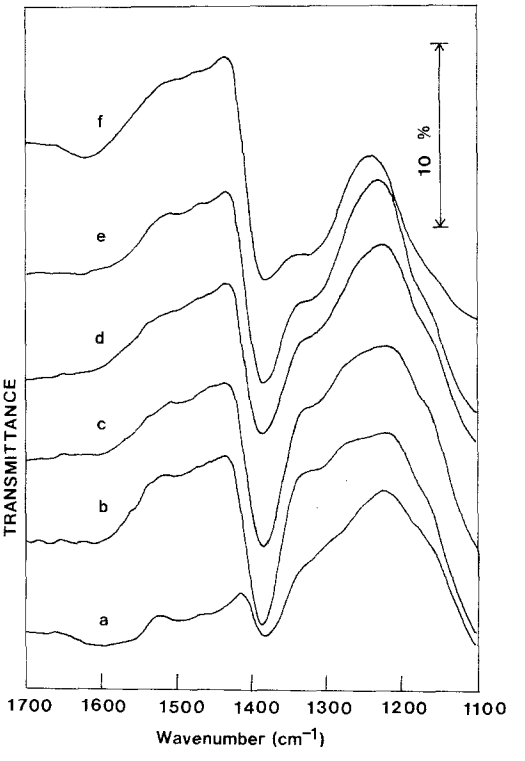

FIG. 3. IR spectra of alumina modified with sulfate: (a) Al–S(1), (b) Al–S(2), (c) Al–S(3), (d) Al–S(4), (e) Al–S(5), and (f) Al–S(10). Pretreatment condition: evacuated at 773 K and for 2 h.

IR

The IR spectra of Al–S are shown in Fig. 3. An IR band at 1383 cm^{-1} was observed when Al–S(1) was calcined at 773 K, which may be assigned to the asymmetric stretching band of the S=O group (*26–28*). Another IR band at 1330 cm^{-1} appeared and its intensity increased with increasing sulfate content.

The IR spectra of pure alumina and Al–S upon the adsorption of pyridine are shown in Fig. 4. Three IR bands at 1446, 1490, and 1620 cm^{-1} were assigned to pyridine adsorbed on the Lewis acid sites on alumina (*29*). The IR band at 1594 cm^{-1} indicates physisorbed pyridine. The IR bands of pyridine adsorbed on Al–S(1) and Al–S(5) were similar to those on pure alumina. A new IR band at 1549 cm^{-1} appeared in Al–S(10), indicating the presence of pyridine adsorbed on the Brønsted acid site (*29, 30*). The IR spectrum of pyridine adsorbed on Al–P(10) was similar to that adsorbed on alumina as shown in Fig. 4(e). The IR band at 1549 cm^{-1}, which was observed in Al–S(10), did not appear.

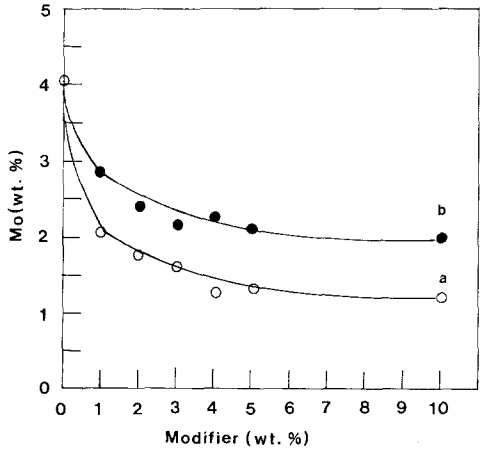

FIG. 2. The Mo uptake on alumina modified with various contents of modifier: (a) Al–S and (b) Al–P.

DRS

Figure 5 shows the DRS spectra of the Mo catalysts calcined at 773 K. Two bands

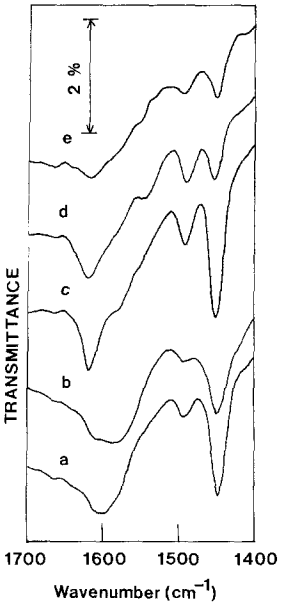

FIG. 4. IR spectra of pyridine adsorbed on modified alumina: (a) pure alumina, (b) Al–S(1), (c) Al–S(5), (d) Al–S(10), and (e) Al–P(10). Pretreatment condition: pyridine was adsorbed at 423 K for 2 h followed by the evacuation at the same temperature for 2 h.

were observed at 220 and 260 nm in Mo/Al_2O_3. In Mo/Al–S a new band appeared at 320 nm and its intensity increased with increasing sulfate content as shown in Fig. 5(A). The band at 220 nm has been assigned to the tetrahedral Mo species while the band at 320 nm has been assigned to the octahedral Mo species (*16, 31, 32*). The band at 320 nm also increased with increasing phosphate content in Mo/Al–P as shown in Fig. 5(B).

XRD

There was no evidence for bulk MoO_3 in Mo/Al_2O_3, nor did the XRD patterns of bulk MoO_3 appear in the Mo/Al–P sample with a phosphate content below 5 wt%. In Mo/Al–P(10) weak XRD patterns appeared around $2\theta = 26°$ assigned to bulk MoO_3 (*33*). The XRD patterns due to bulk MoO_3 began to appear around $2\theta = 26°$ in Mo/Al–S with a sulfate content of 5 wt%. The XRD patterns around $2\theta = 29°$ and 47°, which originate from crystalline MoO_3 (*33*), were observed in Mo/Al–S(10) with an intensity higher than that of Mo/Al–P. Bulk MoO_3 was formed more easily on Al–S than on Al–P.

ESR

The ESR spectra of Mo catalysts sulfided at 673 K for 2 h are shown in Fig. 6. ESR band I ($g = 1.93$) has been assigned to Mo^{+5} coordinated to oxygen, which is stabilized to alumina (*34, 35*), while ESR band II ($g = 2.02$) has been assigned to Mo species in sulfur environments such as thio-Mo^{+5} species located at the edge sites of MoS_2 phase (*34*) or the bulk defects in a MoS_2-like phase (*36*). The intensities of ESR band I of sulfided Mo/Al–S and Mo/Al–P were weaker than that of sulfided Mo/Al_2O_3. The intensity of ESR band I decreased considerably when 1 wt% of sulfate or phosphate was added. When the content of modifier was

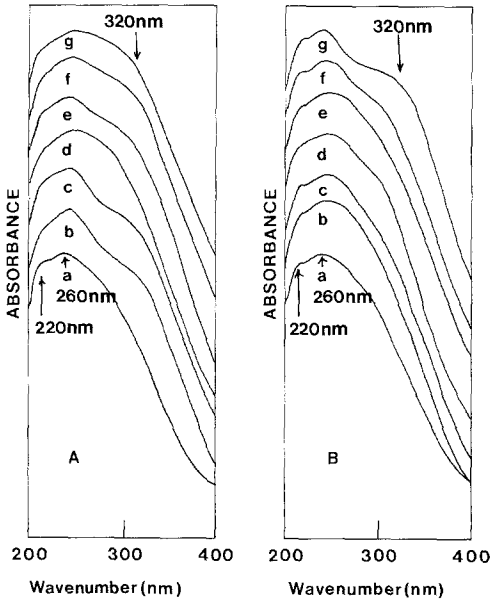

FIG. 5. DRS spectra of Mo catalysts calcined at 773 K: (A) (a) Mo/Al_2O_3; (b) Mo/Al–S(1); (c) Mo/Al–S(2); (d) Mo/Al–S(3); (e) Mo/Al–S(4); (f) Mo/Al–S(5); and (g) Mo/Al–S(10). (B) (a) Mo/Al_2O_3; (b) Mo/Al–P(1); (c) Mo/Al–P(2); (d) Mo/Al–P(3); (e) Mo/Al–P(4); (f) Mo/Al–P(5); and (g) Mo/Al–P(10).

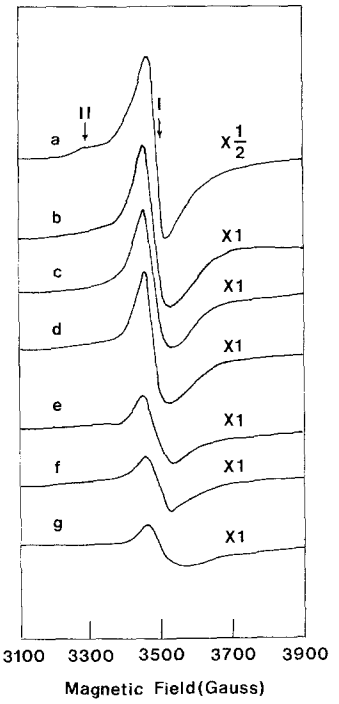

FIG. 6. ESR spectra of Mo catalysts sulfided at 673 K: (a) Mo/Al_2O_3, (b) Mo/Al–P(1), (c) Mo/Al–P(5), (d) Mo/Al–P(10), (e) Mo/Al–S(1), (f) Mo/Al–S(5), and (g) Mo/Al–S(10).

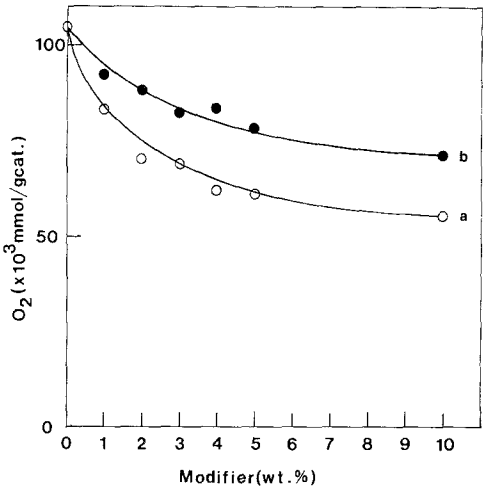

FIG. 7. The amount of oxygen chemisorbed on Mo catalysts sulfided at 673 K: (a) Mo/Al–S and (b) Mo/Al–P.

above 1 wt%, the intensity of ESR band I slightly decreased. The intensity of ESR band I in Mo/Al–S was weaker than that of ESR band I in Mo/Al/P.

Oxygen Chemisorption

Figure 7 shows that the amount of oxygen chemisorbed on Mo/Al–S and Mo/Al–P sulfided at 673 K decreased with increasing modifier content. The amount of oxygen chemisorbed on Mo/Al–S was less than that of oxygen chemisorbed on Mo/Al–P.

Temperature-Programmed Sulfidation

The TPS spectra of Mo/Al_2O_3 are shown in Fig. 8. There are two regions of H_2S consumption: below 500 K (region I) and above 600 K (region II). H_2S production accompanied by a H_2 consumption occurred between 500 and 600 K. H_2O production began to occur at 550 K and reached a maximum at 820 K as shown in Fig. 8(c). There were two contradictory reports that H_2O production and H_2S consumption occur simultaneously (*24*) and that H_2O production occurs following onset of the signal of H_2S consumption

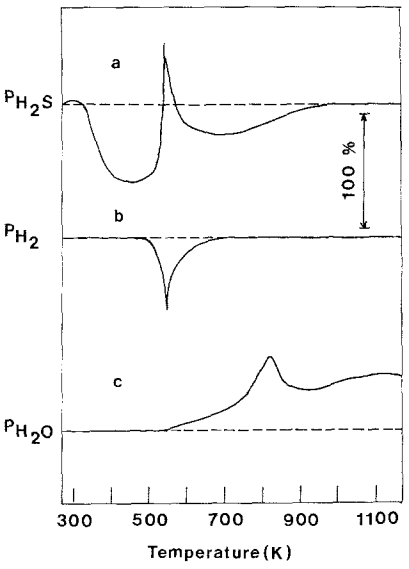

FIG. 8. TPS pattern of Mo/Al_2O_3: (a) H_2S, (b) H_2, and (c) H_2O. The arrow indicates the intensity of H_2S pressure when 100% of H_2S was consumed during TPS.

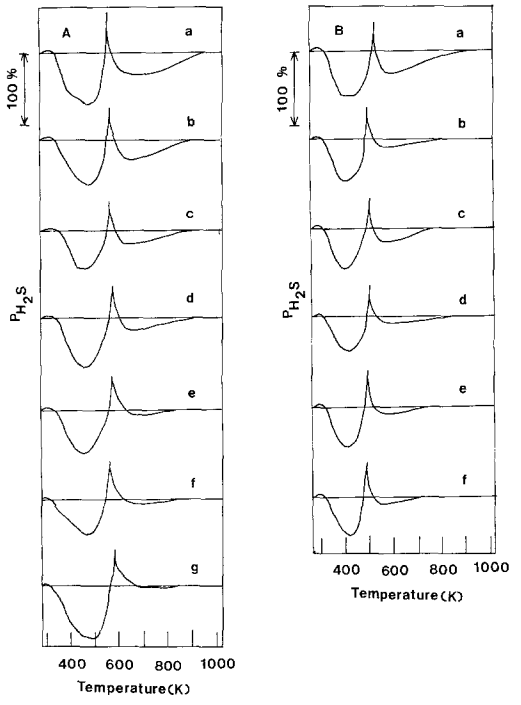

FIG. 9. TPS patterns (H_2S) of Mo catalysts: (A) (a) Mo/Al_2O_3; (b) Mo/Al–S(1); (c) Mo/Al–S(2); and (d) Mo/Al–S(3); (e) Mo/Al–S(4); (f) Mo/Al–S(5); and (g) Mo/Al–S(10). (B) (a) Mo/Al–P(1); (b) Mo/Al–P(2); (c) Mo/Al–P(3); (d) Mo/Al–P(4); (e) Mo/Al–P(5); and (f) Mo/Al–P(10).

(*37*). The H_2O signal, which remained above 950 K without a concurrent change in the H_2S and H_2 signals, originates from the dehydration of alumina, because the sample was calcined only at 773 K before TPS. The color of the Mo catalyst changed from yellowish-white to grayish black due to the adsorption of H_2S during stabilization at room temperature. The H_2S adsorbed on the Mo catalyst desorbed below 373 K without H_2O production.

Figure 9 shows the variations of the partial pressure of H_2S during TPS of the Mo catalysts. In Mo/Al–P the amount of H_2S consumption in region II decreased with increasing phosphate content. Also the temperature of the maximum H_2S production peak decreased from 550 to 480 K as phosphate content increased to 5 wt% as shown

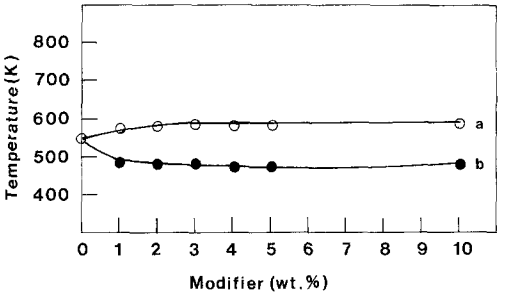

FIG. 10. The maximum temperature of H_2S production vs the modifier content: (a) Mo/Al–S and (b) Mo/Al–P.

in Fig. 10. Although the amount of H_2S consumption in region II also decreased with sulfate content, the maximum H_2S production peak temperature shifted from 550 to 590 K when pure alumina was modified with 10 wt% of sulfate.

HDS Activity

The activities in the thiophene HDS with Mo/Al–S and Mo/Al–P are shown in Fig. 11. The HDS activity of Mo/Al–P samples with less than 5 wt% phosphate was higher than that of Mo/Al_2O_3, while the HDS activity of Mo/Al–P(10) was lower than that of

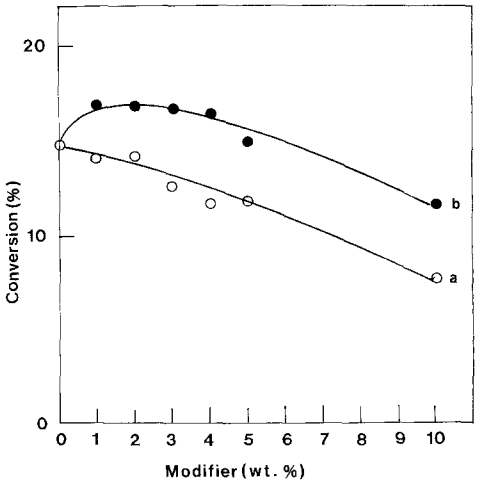

FIG. 11. The thiophene HDS conversion of Mo catalysts: (a) Mo/Al–S and (b) Mo/Al–P.

Mo/Al_2O_3. The HDS activity of Mo/Al–S was lower than that of Mo/Al_2O_3 and decreased with increasing sulfate content.

DISCUSSION

Bonding Mode of Sulfate

When the alumina was modified with sulfate, two IR bands at 1383 and 1330 cm^{-1} were observed as shown in Fig. 3. The intensity of the IR band at 1330 cm^{-1} increased with increasing sulfate content. The band at 1383 cm^{-1} is assigned to the asymmetrical stretching band of the S=O group (*26–28*). The IR band at 1330 cm^{-1} is a characteristic of the S=O group (*26–28*) and has been related with association with H_2O or with surface hydroxyl groups (*26, 38*). The IR band at 1330 cm^{-1} appeared at relatively high sulfate content without water being added in our IR spectra, which shows that the bonding mode of sulfate can be affected according to the sulfate content. The sulfate is multidentately (*26, 27, 39*) bonded to the alumina surface modified with a low sulfate content. The amount of the hydroxyl groups on the alumina surface decreases as the sulfate content increases. Therefore, the amount of monodentately bonded sulfate increases with increasing sulfate content.

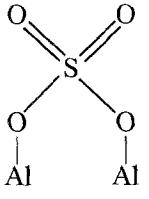

(I)

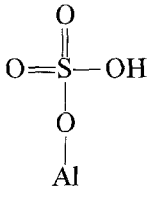

(II)

The monodentately bonded sulfate has a free S–OH group. The S=O bond in the sulfate group has an electron-withdrawing character resulting in a reduction of the electron density of its chemical environment (*27, 28*). Therefore, the monodentately bonded sulfate might change to mode (III), which has the character of the partial double bond of the S=O group. The appearance of the IR band at 1330 cm^{-1} might be explained by the bonding mode (III).

TABLE 2

Final pH of Mo Solution after the Adsorption Experiment

Support	pH	PZC	Support	pH	PZC
Al_2O_3	4.71	8.3	—		
Al–P(1)	4.67	7.6	Al–S(1)	4.64	6.1
Al–P(4)	4.64	6.7	Al–S(4)	4.35	4.3
Al–P(10)	4.63	6.5	Al–S(10)	4.26	3.5

Note. The pH of initial Mo solution was 4.41.

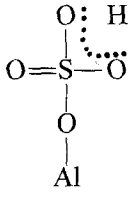

(III)

Upon adsorption of pyridine on Al–S(10) (Fig. 4) an IR absorbtion band appeared at 1549 cm^{-1}. This Brønsted acid site can originate either from the hydroxyl group in sulfate or from the hydroxyl groups on the alumina. The number of the hydroxyl groups on the alumina surface decreases with increasing sulfate content, because the hydroxyl groups on the alumina were consumed via a reaction with the hydroxyl group in sulfate. Therefore, it is more likely that the Brønsted acid site in Al–S(10) originates from the hydroxyl group in sulfate (mode (III)).

Mo Catalyst Supported on Alumina Modified with Phosphate

As shown in Table 2, the final pH of Mo solution after the Mo adsorption experiment increased toward the PZC of pure alumina. Similar results were previously reported because of the buffer capacity of the alumina as explained in the equilibrium (*4, 15, 40*)

$$AlOH + H(sol)^+ \rightleftharpoons AlOH_2^+ \quad (a)$$

($H_{(sol)^+}$: hydrogen ion (or proton) in bulk solution).

The increase in pH of Mo solution increases the concentration of the monomeric Mo anion because the polymeric $Mo_7O_{24}^{-6}$ and monomeric MoO_4^{-2} are in equilibrium, as denoted in

$$7MoO_4^{-2} + 8H^+ \rightleftharpoons Mo_7O_{24}^{-6} + 4H_2O. \quad (b)$$

Below pH 5 Mo anions exist as polymeric Mo anions such as $Mo_7O_{24}^{-6}$ and $Mo_8O_{26}^{-4}$ while above pH 9 Mo is present as monomeric MoO_4^{-2} (*41*).

When the phosphate is added on the alumina, final pH decreases upon increasing phosphate content (Table 2). These results show that the tendency of the alumina to electrostatically adsorb the $H_{(sol)^+}$ in Mo solution is limited when the alumina is modified with phosphate. Therefore, the concentration of $H_{(sol)^+}$ in Mo solution is higher for Al–P than for Al_2O_3. This causes the equilibrium of Eq. (b) to shift to the right and the amount of the polymeric Mo anion increases in the Mo solution. The pH of the impregnation solution near the support surface changed toward the PZC of the support (*42*). Therefore, the adsorption of the polymeric Mo anion is more likely, compared to that of the monomeric Mo anion, when the alumina surface is modified with the phosphate.

The deposition of Mo anion occurs simultaneously both by the adsorption and the precipitation during the preparation of the Mo catalyst by incipient wetness method. The adsorption of the Mo anions occurs on the protonated hydroxyl groups of the alumina surface (*4–7*), the concentration of which may be controlled by the dopants (*9, 10*). Moreover the change in PZC of the support surface is known to influence the adsorption of Mo anion on the support (*6–11, 41*). As shown in Fig. 1, the addition of phosphate decreased the PZC of the alumina, which decreases the number of adsorption site for the Mo anions (Fig. 2).

When alumina was modified with the phosphate, an $AlPO_4$-like structure is known to be formed (*14, 18, 19, 43*). IR studies have shown the existence of the interaction between Mo and the $AlPO_4$-like structure (*14, 19*). There are fewer adsorption sites for Mo anion on the phosphated alumina surface than on pure alumina surface (*14*). Therefore, the formation of the $AlPO_4$-like structure contributes to the decrease in the adsorption sites for the Mo anions. The decrease in the PZC and the formation of the $AlPO_4$-like structure suggest that less Mo deposition by the adsorption process occurs on the phosphated than on pure alumina surface. Also the modification of the alumina surface by phosphate results in the decrease in the surface area of the alumina support shown in Table 1. As a result during the impregnation, the Mo deposition by adsorption process decreases.

When the phosphate is added on the alumina surface, the change in the electrical and textural properties of the support affect the amount of the adsorption sites for the Mo anions and the types of Mo species in Mo solution. The amount of Mo deposition by the adsorption process decreases and the concentration of polymeric Mo anion in the Mo solution increases, thus resulting in the increase in the amount of the polymolybdate on Al–P. This suggestion is supported by the DRS results, which show that the intensity of the DRS band at 320 nm, originating from the octahedral molybdate, increased with increasing phosphate content (Fig. 5). Previous TPR study also indicates that the higher fraction of reducible octahedrally coordinated Mo species was found in Mo catalyst supported on phosphated alumina (*16*).

The modification of alumina with phosphate can influence the sulfidation of molybdate. When calcined Mo catalyst was isothermally sulfided at 673 K, the intensity of ESR band I ($g = 1.93$) in Mo/Al–P was weaker than that in Mo/Al_2O_3, indicating that the interaction between Mo and alumina decreased because this band suggests Mo^{+5} species that are stabilized by the alu-

mina and have a tetrahedrally coordinated structure (*34, 35*). The tetrahedral Mo^{+5} stabilized by alumina is sulfided under mild conditions with difficulty because it interacts strongly with alumina (*34*). A decrease in the interaction between Mo and alumina facilitates the sulfidation of molybdate into Mo sulfide (*2, 24, 44*). The TPS result that the amount of molybdate sulfided at the higher sulfidation temperature (region II) decreased with increasing phosphate content, as shown in Fig. 9, indicates that the sulfidation of Mo/Al–P occurred mainly at a lower temperature (region I). In addition, the temperature of maximum H_2S production changed from 550 to 480 K as the phosphate content increased to 5 wt% as shown in Fig. 10. When TPS of Mo/Al_2O_3 calcined at 773 K was carried out, the maximum temperature of H_2S production shifted from 560 to 480 K with increasing Mo loading (*24*). This shift is explained by taking into consideration HDS activity for sulfur reduction per Mo site.

The interaction between Mo and alumina through Mo–O–Al groups remaining after the sulfidation of Mo/Al_2O_3 (*45, 46*) results in the polarization of the Mo–S bonding in Mo sulfide, which in turn decreases the covalent character of the Mo–S bonding. Since a catalyst with a lower covalency of the Mo–S bonding is supposed to have a lower activity (*47*), the higher polarization of the Mo–S bonding by the interaction between Mo and alumina might decrease the HDS activity. When Mo is supported on alumina modified with phosphate, the amount of Mo species stabilized by the alumina decreases as shown in ESR spectra of Fig. 6, indicating that the polarization of the Mo–S bonding in Mo/Al–P is less than that in Mo/Al_2O_3. Therefore, the HDS activity with Mo/Al–P with less than 5 wt% phosphate increased when the thiophene HDS reaction was carried out at 573 K.

Comparison of Al–P(10) with Al–P containing less than 5 wt% of phosphate showed that the PZC and the final pH of the Mo solution after the adsorption did not change significantly while the alumina surface area decreased continuously. The decrease in the surface area might originate from plugging the support pores by phosphate (*16*). In Al–P(10) the textural change in the support surface is more important than the change in the surface charge characteristics. Since the surface area decreases, the amount of the Mo deposition might increase by the precipitation process rather than the adsorption process. These precipitates on the alumina surface contribute to the formation of bulk MoO_3 during calcination. The XRD spectrum of Mo/Al–P(10) shows the appearance of the XRD peak around $2\theta = 26°$ assigned to bulk MoO_3. The formation of bulk MoO_3 contributes to the decrease in the dispersion of Mo sulfide, which was further evidenced by the decrease in the amount of oxygen chemisorption as the phosphate content increased. When the phosphate was added on the alumina before the impregnation of Mo anion, the enrichment of Mo in outer surface of the alumina resulted in large Mo sulfide crystallites (*15, 17*). The decrease in the Mo dispersion decreased the HDS activity. When the thiophene HDS was performed at 673 K, the activity of Mo/Al–P(10) was lower than that of Mo/Al_2O_3.

In summary, when Mo was supported on alumina modified with phosphate, phosphate facilitated the formation of polymolybdate, decreased the number of the interaction site, and facilitated the sulfidation of molybdate into Mo sulfide active for the HDS reaction.

Mo Catalyst Supported on Alumina Modified with Sulfate

A shift of the PZC of alumina to lower pH values would decrease the number of adsorption sites for the anionic species (*6, 7, 26, 48*), suggesting that Al–S(1) possesses fewer adsorption sites as compared with Al–P(10). The fact that the amount of Mo uptake on Al–S(1) was less than that on Al–P(10) is attributed to the decrease in the number of the adsorption sites, because the specific surface area of Al–S(1) was larger

than that of Al–P(10) as shown in Table 1. The PZC of Al–S decreased from 6.1 to 3.4 as the sulfate content increased from 1 to 10 wt%, indicating that the Mo anions adsorbed on Al–S were polymeric rather than monomeric Mo anion.

In the alumina with higher sulfate content, the final pH of Mo solution after the Mo adsorption decreased from 4.41 toward the PZC of Al–S (Table 2). This decrease in pH after the Mo adsorption may be explained by the equilibrium

$$AlOH_2^+ \rightleftharpoons AlOH + H_{(sol)}^+. \qquad (c)$$

The shift of equilibrium (c) to the right may also be responsible for the decrease of the number of the adsorption sites for the Mo anions. As a result, the amount of the Mo deposition by the precipitation process is larger on the alumina modified with sulfate than on the alumina modified with phosphate. The formation of bulk MoO_3 on Al–S is therefore favored. The XRD patterns shown at $2\theta = 26°$, 29°, and 47° confirm the formation of bulk MoO_3.

During TPS (Fig. 9), the amount of H_2S consumed above 500 K before the H_2S production occurred was larger in Mo/Al–S than in Mo/Al_2O_3. This suggests that the amount of molybdate sulfided at a higher temperature is larger in Mo/Al–S than in Mo/Al_2O_3. This may be due to the presence of the electron withdrawing S=O group (*27, 28*), which results in the enhancement of the polar character of the Mo–O bonding in the molybdate species. The polarization of the Mo–O bonding requires a higher temperature for the sulfidation of molybdate (*24*). As a result, the reduction of sulfur may occur at higher temperature (Fig. 10), as it occurs following the sulfidation of molybdate (*24*). The sulfidation of bulk MoO_3 requires a sulfidation temperature higher than the well-dispersed MoO_3 or polymolybdate (*2, 24*).

When the thiophene HDS reaction was performed at 573 K, the HDS activity of Mo/Al–S catalyst was lower than the activity of Mo/Al_2O_3. The lower HDS activity of Mo/Al–S is due to the decrease in the Mo dispersion in sulfided Mo/Al–S catalyst, which is supported by the oxygen chemisorption result that showed that less oxygen was chemisorbed on sulfided Mo/Al–S (Fig. 7). The formation of bulk MoO_3 on Mo/Al–S contributes to the decrease in the Mo dispersion. The ESR spectra showing that the intensity of ESR band I, corresponding to the interaction between Mo^{+5} and alumina, was weaker in Mo/Al–S than in Mo/Al_2O_3, indicating that these Mo^{+5} species are formed less in Mo/Al–S than in Mo/Al_2O_3. The decrease in the amount of Mo^{+5} species that may be located at the edge of the MoS_2 resulting in their stabilization toward growth (*34*) may facilitate the formation of large Mo–sulfide crystallites.

Because of the electron-withdrawing character of the S=O group (*26–28*), the Mo–S bonding is polarized, resulting in the decrease in the covalency of the Mo–S bonding. The decrease of the electron density on the Mo–S bonding decreases the HDS activity (*47*). Similarly, it has been suggested that the promoting activity of Co and Ni may be ascribed to the ability to donate electrons to Mo, while the poisoning activity of Cu may be ascribed to the electron withdrawal (*49*). In summary, the formation of bulk MoO_3 and the presence of the S=O group may explain the decrease in the HDS activity in Mo/Al–S when the thiophene HDS reaction was carried out at 573 K (Fig. 11).

ACKNOWLEDGMENT

One of authors (S. I. Kim) is grateful to the fellowship awarded by Ssang-yong Oil Refinery Company (Korea).

REFERENCES

1. Massoth, F. E., *in* "Advances in Catalysis" (D. D. Eley, H. Pines, and P. B. Weisz, Eds.), Vol. 27, p. 265. Academic Press, New York, 1978.
2. Scheffer, B., Arnoldy, P., and Moulijn, J. A., *J. Catal.* **112,** 516 (1988).
3. Candia, R., Topsoe, H., and Clausen, B. S., *in* "Proceedings, 9th Iberinoamerica Symposium on Catalysts, Lisbon, Portugal, 1984," p. 211.
4. van Veen, J. A. R., Hendriks, P. A. J. M., Romes, E. J. G. M., and Andrea, R. R., *J. Phys. Chem.* **94,** 5275 (1990).

5. Mensch, C. T. J., van Veen, J. A. R., van Wingerden, B., and Van Dijk, M. P., *J. Phys. Chem.* **92,** 4961 (1988).
6. Spanos, N., Vordonis, L., Kordulis, Ch., and Lycourghiotis, A., *J. Catal.* **124,** 301 (1990).
7. Spanos, N., Vordonis, L., Kordulis, Ch., and Lycourghiotis, A., *J. Catal.* **124,** 315 (1990).
8. Vordonis, L., Koutsoukos, P. G., and Lycourghiotis, A., *Langmuir* **2,** 281 (1986).
9. Vordonis, L., Koutoukos, P. G., and Lycourghiotis, A., *J. Catal.* **98,** 296 (1986).
10. Vordonis, L., Koutsoukos, P. G., and Lycourghiotis, A., *J. Catal.* **101,** 186 (1986).
11. Mulcahy, F. M., Houalla, M., and Hercules, D. M., *J. Catal.* **106,** 210 (1987).
12. Mulcahy, F. M., Houalla, M., and Hercules, D. M., *in* "Proceedings, 9th International Congress on Catalysis, Calgary, 1988" (M. J. Phillips and M. Ternan, Eds.), p. 1968. Chem. Institute of Canada, Ottawa, 1988.
13. Mieth, J. A., Schwarz, J. A., Huang, Y. J., and Fung, S. C., *J. Catal.* **122,** 202 (1990).
14. van Veen, J. A. R., Hendriks, P. A. J. M., Andrea, R. R., Romers, E. J. G. M., and Wilson, A. E., *J. Phys. Chem.* **94,** 5282 (1990).
15. Cheng, W. C., and Luthra, N. P., *J. Catal.* **109,** 163 (1988).
16. Lopez Cordero, R., Esquivel, N., Lazaro, J., Fierro, J. L. G., and Lopez Agudo, A., *Appl. Catal.* **48,** 341 (1989).
17. Fierro, J. L. G., Lopez Agudo, A., Esquivel, N., and Lopez Cordero, R., *Appl. Catal.* **48,** 353 (1989).
18. Lopez Cordero, R., Lopez Guerra, S., Fierro, J. L. G., and Lopez Agudo, A., *J. Catal.* **126,** 8 (1990).
19. Mangnus, P. J., van Veen, J. A. R., Eijsbouts, S., de Beer, V. H. J., and Moulijn, J. A., *Appl. Catal.* **61,** 99 (1990).
20. Atanasova, P., Halachev, T., Uchytil, J., and Kraus, M., *Appl. Catal.* **38,** 235 (1988).
21. Fitz, C. W., Jr., and Rase, H. F., *Ind. Eng. Chem. Prod. Res. Dev.* **22,** 40 (1983).
22. Morales, A., Ramirez de Agudelo, M. M., and Hernandez, F., *Appl. Catal.* **41,** 261 (1988).
23. Kim, J. C., and Woo, S. I., *Appl. Catal.* **39,** 107 (1988).
24. Arnoldy, P., van den Heikant, J. A. M., de Bok, G. D., and Moulijn, A., *J. Catal.* **92,** 35 (1985).
25. Scheffer, B., de Jonge, J. C. M., Arnoldy, P., and Moulijn, J. A., *Bull. Soc. Chim. Belg.* **93,** 751 (1984).
26. Saur, O., Bensitel, M., Mohammed Saad, A. B., Lavalley, J. C., Tripp, C. P., and Morrow, B. A., *J. Catal.* **99,** 104 (1986).
27. Jin, T., Yamaguchi, T., and Tanabe, K., *J. Phys. Chem.* **90,** 4794 (1986).
28. Yamaguchi, T., Jin, T., and Tanabe, K., *J. Phys. Chem.* **90,** 3148 (1986).
29. Kiviat, F. E., and Petrakis, L., *J. Phys. Chem.* **77,** 1232 (1973).
30. Przystajko, W., Fiedorow, R., and Dalla Lana, I. G., *Appl. Catal.* **15,** 265 (1985).
31. Jeziorowski, H., and Knozinger, H., *J. Phys. Chem.* **83,** 1166 (1979).
32. Gil Llambias, F. J., Mendioroz, S., Ania, F., and Lopez Agudo, A., *Appl. Catal.* **8,** 335 (1983).
33. Gajardo, P., Grange, P., and Delmon, B., *J. Phys. Chem.* **83,** 1771 (1979).
34. Derouane, E. G., Pedersen, E., Clausen, B. S., Gabelica, Z., Candia, R., and Topsoe, H., *J. Catal.* **99,** 253 (1986).
35. Bhaduri, M., Hernandez, J., and Thomas, W. J., *Appl. Catal.* **8,** 85 (1983).
36. Konings, A. J. A., Brentjens, W. L. J., Koningsberger, D. C., and de Beer, V. H. J., *J. Catal.* **67,** 145 (1981).
37. Stuchly, V., Zahradnikova, H., and Beranek, I., *Appl. Catal.* **35,** 23 (1987).
38. Kayo, A., Yamaguchi, T., and Tanabe, K., *J. Catal.* **83,** 99 (1983).
39. Okamoto, Y., and Imanaka, T., *J. Phys. Chem.* **92,** 7102 (1988).
40. van Veen, J. A. R., de Wit, H., Emeis, C. A., and Hendriks, P. A. J. M., *J. Catal.* **107,** 579 (1987).
41. Wang, L., and Keith Hall, W., *J. Catal.* **77,** 232 (1982).
42. Luthra, N. P., and Cheng, W. C., *J. Catal.* **107,** 154 (1987).
43. Stanislaus, A., Absi-halabi, M., and Al-dolama, K., *Appl. Catal.* **39,** 239 (1988).
44. Kim, S. I., and Woo, S. I., *Appl. Catal.* **74,** 109 (1991).
45. Schrader, G. L., and Cheng, C. P., *J. Catal.* **80,** 369 (1983).
46. Candia, R., Sorensen, O., Villadsen, J., Topsoe, N. Y., Clausen, B. S., and Topsoe, H., *Bull. Soc. Chim. Belg.* **93,** 763 (1984).
47. Harris, S., and Chianelli, R. R., *J. Catal.* **86,** 400 (1984).
48. Brunelle, J. P., *Pure. Appl. Chem.* **50,** 1211 (1978).
49. Harris, S., and Chianelli, R. R., *J. Catal.* **98,** 17 (1986).